

SCLAIR : Supervised Contrastive Learning for User and Device Independent Airwriting Recognition

Ayush Tripathi¹, Arnab Kumar Mondal², Lalan Kumar^{1,3}, Prathosh A.P.⁴

¹Department of Electrical Engineering, Indian Institute of Technology Delhi, New Delhi, India

²Amar Nath and Shashi Khosla School of Information Technology, Indian Institute of Technology Delhi, New Delhi, India

³Bharti School of Telecommunication, Indian Institute of Technology Delhi, New Delhi, India

⁴Department of Electrical Communication Engineering, Indian Institute of Science, Bengaluru, India

Abstract—Airwriting Recognition is the problem of identifying letters written in free space with finger movement. It is essentially a specialized case of gesture recognition, wherein the vocabulary of gestures corresponds to letters as in a particular language. With the wide adoption of smart wearables in the general population, airwriting recognition using motion sensors from a smart-band can be used as a medium of user input for applications in Human-Computer Interaction. There has been limited work in the recognition of in-air trajectories using motion sensors, and the performance of the techniques in the case when the device used to record signals is changed has not been explored hitherto. Motivated by these, a new paradigm for device and user-independent airwriting recognition based on supervised contrastive learning is proposed. A two stage classification strategy is employed, the first of which involves training an encoder network with supervised contrastive loss. In the subsequent stage, a classification head is trained with the encoder weights kept frozen. The efficacy of the proposed method is demonstrated through experiments on a publicly available dataset and also with a dataset recorded in our lab using a different device. Experiments have been performed in both supervised and unsupervised settings and compared against several state-of-the-art domain adaptation techniques. Data and the code for our implementation will be made available at <https://github.com/ayushayt/SCLAIR>.

Index Terms—Airwriting, Smart-band, Wearables, Supervised Contrastive Learning, Domain Adaptation.

I. INTRODUCTION

A. Background

Airwriting may be defined as the process of writing letters in free space using unrestricted finger movements [1], [2]. It can be used to provide a user with a fast and touch-less input option which can be employed for applications in Human-Computer Interaction [3]. The recognition of writing from motion sensors has garnered attention over the past few years and numerous algorithms have been proposed for the task [4]–[10]. The studies involving the use of motion sensors can be broadly divided into two categories, the first involving the use of dedicated devices such as a wearable glove [11], Wii remote [12]–[14], smartphone [15] and vision-based [16]. This approach however, involves the user to carry an extra physical device which may be cumbersome for the users. To mitigate this, the second category of approaches aim to recognize writing movements by using wearable devices such as a ring worn on the index finger [17], smart-bands [18].

B. Related Work

There have been several attempts made at recognizing gestures of the palm by using wrist-worn devices [19], [20]. However, most of the work around this area has been focused on the setting wherein a stable, flat surface is used during the writing process [21]–[23]. The presence of a flat surface for writing leads to stabilization of the hand, thereby decreasing noise and also provides a degree of feedback to the user. Close to the current work, in [24] the authors explored the problem of airwriting recognition using a wrist-worn device. The study involved a single participant and Dynamic Time Warping (DTW) was used as a distance measure for classification thereby

making the study user dependent. In [18], the authors have proposed a Convolutional Neural Network based user independent framework in addition to a DTW based user dependent method for recognizing airwritten English uppercase alphabets. While all these methods are shown effective in airwriting recognition, they are limited in terms of user and device dependent nature of the studies performed hitherto. Such a system has the drawback of not generalizing to large-scale population due inter-subject variability in writing the same character. Furthermore, difference in the acquisition sensor characteristics across different devices may prove to be detrimental for the performance of airwriting recognition systems. Motivated by this, the current study explores a new paradigm for both user and device independent recognition of airwritten alphabets using signals obtained from 3-axis accelerometer and gyroscope sensors.

C. Objectives and Contributions

In this work, we explore a supervised contrastive learning [25] based architecture for airwriting recognition. The main idea behind the approach is that the hidden representations of signals for the same alphabet are expected to be similar to each other, while the representation corresponding to signals of different alphabets will be fairly different. Given this intuition, a 2-stage classification approach is adopted wherein, in the first stage, an encoder (with a projection head) is trained with using the contrastive loss. Subsequently, the projection head is discarded and a classification head is trained while keeping the encoder weights fixed. We validate the efficacy of the proposed approach by performing leave-one-subject-out experiments on 2 different datasets - a publicly available dataset [18] (source dataset) and a dataset collected in the lab (target dataset). We also analyze the performance of the approach in two different settings, (a) an unsupervised setting in which the model is trained solely

using the source domain data and evaluated on the target domain samples, and (b) a supervised setting in which the encoder is trained using source domain samples and the classifier head is fine tuned using target domain samples. We demonstrate that the supervised contrastive learning based approach leads to improved recognition accuracy on the target dataset, compared to other domain adaptation techniques - DANN [26] , DRCN [27] and DeepJDOT [28] in both supervised and unsupervised settings.

II. PROPOSED METHOD

The proposed framework consists of two stages, an encoder network trained using contrastive loss and a subsequent classifier head trained using the cross-entropy loss. Figure 1 depicts the overall network.

A. Problem Description

A multivariate time-series recorded using 3-axis accelerometer and gyroscope of an Inertial Measurement Unit (IMU) placed on the wrist of the dominant hand of a human subject while writing uppercase English alphabets forms the input for the method. The signal is recorded over three axes (X, Y and Z), resulting in a total of six time series for each sample. Suppose we have a batch of N sample and label pairs represented as $\{x_k, y_k\}_{k=1,2,\dots,N}$ where $x_k \in \mathcal{X}$ is the input time series corresponding to the alphabet $y_k \in \{A, B, \dots, Z\}$. The encoder network, $Enc(\cdot) : \mathcal{X} \rightarrow R^{D_E}$ maps the input x to a D_E dimensional representation vector $r = Enc(x)$. Subsequently, the vector r is normalized to unit hypersphere in R^{D_E} . There can be various choices of the encoder architecture that can be adopted without any constraints. Subsequently, the projection head maps the encoded representation r to a vector $z = Proj(r) \in R^{D_p}$. This comprises of the first stage of the training and involves learning the parameters of the encoder along with the projection head which is done by minimizing the supervised contrastive loss. It is to be noted that at the end of this stage of training, the projection network is discarded while the encoder weights are retained.

The second stage is the classifier $C(\cdot)$ which is a mapping from the latent space obtained from the encoder (r) to different alphabets. The predicted output is therefore given by $\hat{y} = C(r) = \sigma(W^T r)$. Here, W is the classifier weight matrix and $\sigma(\cdot)$ is the softmax activation function. Since, the projection head is discarded after Stage 1 of the training process, at inference-time, the overall model has the same number of parameters as a standard classification model trained using Cross-Entropy Loss.

B. Supervised Contrastive Loss

Let $i \in I \equiv \{1, 2, \dots, N\}$ be index of an arbitrary sample from a batch of the training dataset, $P(i)$ be the set of indices of samples belonging to the same class as the i^{th} sample in the batch and $A(i) \equiv I \setminus \{i\}$ be the set of indices of all samples from the batch other than the i^{th} sample and $z_i = Proj(Enc(x_i))$ be the output of the projector head for input sample x_i . Supervised contrastive loss [25] is defined as,

$$L^{sup} = \sum_{i \in I} \frac{-1}{|P(i)|} \sum_{p \in P(i)} \log \frac{\exp(\frac{z_i \cdot z_p}{\tau})}{\sum_{a \in A(i)} \exp(\frac{z_i \cdot z_a}{\tau})} \quad (1)$$

In the above equation, τ is a scalar temperature parameter and $x \cdot y$ represents the inner product between vectors x and y . Minimizing the aforementioned loss function encourages the encoder to learn closely aligned representation vectors for samples belonging to the

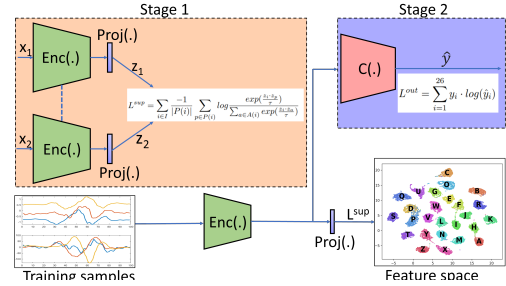


Fig. 1: Block diagram depicting our method. In the first stage an encoder with projection head based on deep network (called $Enc(\cdot)$ and $Proj(\cdot)$ respectively) is trained using supervised contrastive loss. Next, the projection head is discarded and a linear classifier ($C(\cdot)$) is cascaded on top of the feature learner and trained with Cross Entropy loss. The dashed lines indicate that the encoders have shared weights.

same class by using the inner product as a measure of similarity between samples. The gradient of the loss function with respect to z_i can be computed as

$$\frac{\delta L_i^{sup}}{\delta z_i} = \frac{1}{\tau} \left\{ \sum_{p \in P(i)} z_p \left(P_{ip} - \frac{1}{|P(i)|} \right) + \sum_{n \in N(i)} z_n P_{in} \right\} \quad (2)$$

Here, $N(i)$ is the set of indices of samples not belonging to the same class as the i^{th} sample in the batch, and $P_{ix} = \exp(z_i \cdot z_x / \tau) / \sum_{a \in A(i)} \exp(z_i \cdot z_a / \tau)$. It can be shown that easier positive and negative pairs have small contribution towards the gradient compared to hard positive and negative pairs that have a larger contribution, giving rise to intrinsic hard positive/negative mining.

C. Model Architecture

We explore the following different architectures for the Encoder block. Ablations on the hyperparameters for different encoder architectures can be seen in Figures 5b & 6 (Supplementary Material).

- 1) 1DCNN : The architecture comprises of 4 convolutional layers interleaved by a pooling layer, and followed by a Global Average Pooling layer. For the first couple of convolution layers, the number of filters is set to be 100 while in the later stage at 160, while the filter length for each of the layers is 10.
- 2) LSTM and BiLSTM : Here, vanilla LSTM and BiLSTM with 256 number of units are used.
- 3) 1DCNN-LSTM/BiLSTM : Here, the input signal is passed through a couple of 1D Convolutional layers, followed by a pooling layer and the extracted features are then fed to a 256 unit LSTM/BiLSTM layer. The specifications of the convolutional layers are same as that of the first layers as used in the 1DCNN based encoder.

The projection head is taken to be a single layer comprising of 128 neurons, activated by the ReLU activation function. The parameters of the encoder and the projection head are learned by minimizing the supervised contrastive loss using the Adam optimizer. Further, the final classifier network is a single fully-connected layer comprising of 26 neurons, and activated by softmax activation function with 50% dropout. The classification network is trained using the usual cross Entropy Loss. The effect of varying the projection head dimension and the temperature parameter τ is presented in Figure 5a (cf. Supp.).

III. EXPERIMENTS AND RESULTS

A. Datasets

- Source Dataset** - We use the publicly available dataset from [18] that consists of recordings obtained from 55 subjects (28 female, 27 male; 46 right handed, 9 left handed) while writing English uppercase letters (15 times). A dedicated app was built for the purpose of data collection which the users operated by using their non-dominant hand, while the signals were recorded from 3-axis accelerometer and gyroscope of a Microsoft band 2 worn on the dominant hand. The signals were recorded at the maximum sampling rate of 62 Hz supported by the smart-band.
- Target Dataset** - A dataset consisting of 3-axis accelerometer and gyroscope recordings of 20 subjects (11 male, 9 female) was collected in a lab setting with consent of the participants. A Noraxon Ultium EMG sensor (having an internal IMU) [29] was placed on the wrist of the dominant hand of the participant who was then asked to write the English uppercase letters (repeated 10 times). A user interface built using the Tkinter module in python was used for providing the participant with visual feedback for the letter to be written and also for automating the annotation process of the recordings. In Figure 3 (Supplementary Material), we present the sample data collection setup. The signals were recorded at a sampling rate of 200 Hz as supported by the IMU sensor and later downsampled to 62 Hz in order to match to that of the source dataset. Our data will be made publicly available. Another target dataset comprising of recordings from 10 subjects was recorded using a different device with sampling rate 400 Hz (later downsampled to 62 Hz) with the same experimental setup as described above.

B. Experimental Details

The recorded signals are obtained from different users writing at different speed and character sizes. Therefore the following preprocessing steps were employed.

- 1) The samples are fixed to same length by padding zeros if the length of the sample is less than L (taken to be 155 as in [18]), while discarding the extra samples otherwise.
- 2) To the fix length samples, we apply the usual Z-score normalization for each of the 6 individual signals.

The first set of experiments involves leave-one-subject-out (LOSO) validation on both the source and target datasets to avoid the user bias. The training data in each fold is split into a training set and a validation set having 80:20 ratio. A mini-batch training process with a batch size of 32 is employed and early stopping with a patience of 5 epochs.

In the next set of experiments, Cross Entropy loss based classifier and Supervised Contrastive Loss based classifier have been compared in both supervised and unsupervised settings. In the unsupervised setting, the model is trained on the source dataset and evaluated on the target dataset. In the supervised case, the classifier head is fine tuned using the labelled target dataset in a LOSO fashion. The proposed approach has been compared with different domain adaptation techniques, by using the public implementations of the algorithms - DANN, DRCN and DeepJDOT.

Table 1: Mean recognition accuracy for leave-one-subject-out experiment on source dataset

Architecture	CE	SCL
1DCNN	0.8441	0.8620
LSTM	0.8298	0.8446
BiLSTM	0.8460	0.8760
1DCNN-LSTM	0.8480	0.8723
1DCNN-BiLSTM	0.8592	0.8805

Table 2: Mean recognition accuracy for leave-one-subject-out experiment on target dataset

Architecture	CE	SCL
1DCNN	0.8365	0.8619
LSTM	0.7901	0.7928
BiLSTM	0.8015	0.8384
1DCNN-LSTM	0.8307	0.8455
1DCNN-BiLSTM	0.8269	0.8619

Table 3: Mean recognition accuracy on target dataset in the unsupervised setting

Architecture	DANN	DeepJDOT	DRCN	CE	SCL
1DCNN	0.7569	0.7898	0.7583	0.7617	0.8030
LSTM	0.7519	0.7463	0.7248	0.7440	0.7744
BiLSTM	0.7619	0.6557	0.7576	0.7840	0.8128
1DCNN-LSTM	0.7336	0.6809	0.7296	0.7296	0.7754
1DCNN_BiLSTM	0.7575	0.6588	0.7500	0.7757	0.8053

Table 4: Mean recognition accuracy on target dataset in the supervised setting

Architecture	DANN	DeepJDOT	DRCN	CE	SCL
1DCNN	0.7775	0.7921	0.7713	0.8240	0.8528
LSTM	0.7746	0.7273	0.7536	0.8178	0.8029
BiLSTM	0.7909	0.7151	0.7746	0.8207	0.8565
1DCNN-LSTM	0.7685	0.6853	0.7520	0.8344	0.8319
1DCNN_BiLSTM	0.7928	0.6463	0.7830	0.8590	0.8653

Table 5: Mean accuracy on target dataset 2 without fine-tuning

Architecture	CE	SCL
1DCNN	0.9307	0.9581
LSTM	0.8923	0.9007
BiLSTM	0.8850	0.9342
1DCNN-LSTM	0.9392	0.9476
1DCNN-BiLSTM	0.9076	0.9576

Table 6: Mean accuracy on target dataset 2 with fine-tuning

Architecture	CE	SCL
1DCNN	0.9273	0.9573
LSTM	0.9084	0.9130
BiLSTM	0.9088	0.9046
1DCNN-LSTM	0.9342	0.9388
1DCNN-BiLSTM	0.9331	0.9538

C. Results and Comparison

Table 1 lists the performance of different model architectures by using both Cross Entropy (CE) and Supervised Contrastive Loss (SCL) for LOSO experiments with the accuracies averaged across all the subjects. It is seen that the SCL approach outperforms CE based approach for all model architectures. The results obtained by using this approach (Mean accuracy of 88.05%) also outperforms the best reported accuracy 83.2% on the given dataset [18]. It is also seen that the 1DCNN-BiLSTM model performs the best among all the model architectures. This may be attributed to the fact that the features extracted by the convolutional layer are beneficial for predicting the written alphabet. In Table 2, the results of LOSO experiments performed on the target dataset are tabulated with similar trends.

The evaluation of the models on the target domain samples in the unsupervised setting is presented in Table 3. It is seen that in both CE and SCL based models, there is a decrement in the recognition accuracy when compared to the LOSO experiments in which both training and evaluation was done using samples from the target dataset. However, it can be seen that SCL based approach outperforms CE based approach in this scenario as well, thereby motivating the use of the approach for out-of-domain airwriting recognition system in case labeled target dataset is not available. The performance of the approach is also compared against prevalent domain adaptation techniques and it is observed that SCL approach yields superior performance.

Furthermore, in Table 4, we present the results for the set of experiments in which the classifier head is fine tuned using the labeled target dataset. As expected, the recognition accuracies are greatly improved when compared with the unsupervised setting. Also, it is observed that there is a marginal improvement from the LOSO

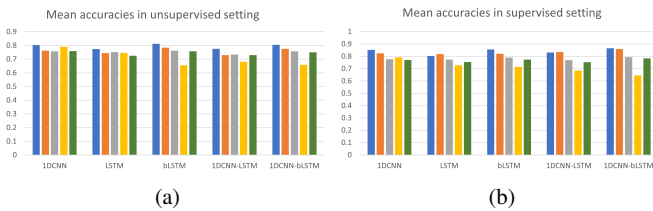


Fig. 2: Mean accuracy on the target dataset using different transfer learning approaches in the (a) unsupervised and (b) supervised setting.

case. The performance of CE and SCL based approaches are found to be quite close while outperforming the baseline domain adaptation techniques. The improvement in the recognition accuracies can be attributed to the fact that the fewer number of parameters are required to be learnt on tuning the classifier head in contrast to learning the parameters for the entire model. Therefore, the encoder parameters learnt on the relatively large source dataset along with the classifier parameters learnt on the small target dataset collectively boost the classification performance. While the trend of improved performance in supervised setting compared to the unsupervised case is in general valid for all the techniques, as illustrated in Figures 2a and 2b the performance of the fine-tuning approach is superior to DANN, DRCN and DeepJDOT. In tables 7 to 10 (Supplementary Material), we present the top-5 most confusing letter pairs for the SCL based approach using the 1DCNN-BiLSTM architecture. In Tables 5 and 6, we present the results of experiments performed by using different device on same subjects without and with fine-tuning. As it can be seen in the tables, SCL based approach outperforms CE based approach in a device-independent but user-dependent study.

IV. CONCLUSION

In this paper, we explored supervised contrastive loss based framework for airwriting recognition using accelerometer and gyroscope signals obtained from a motion sensor worn on the wrist. It is seen that the proposed approach outperforms the state-of-the-art accuracy on a publicly available dataset (source dataset), while also boosting the recognition accuracy on on unseen target dataset. It is seen that the supervised contrastive loss based approach outperforms existing domain adaptation techniques. This implies that our approach can be used for developing an airwriting recognition system, the performance of which is not greatly hampered by variations in the device and user. Future work will focus on exploring explicit methods of bias removal for dataset/user-style specific biases.

REFERENCES

- [1] M. Chen, G. AlRegib, and B.-H. Juang, "Air-writing recognition—part i: Modeling and recognition of characters, words, and connecting motions," *IEEE Transactions on Human-Machine Systems*, vol. 46, no. 3, pp. 403–413, 2016.
- [2] —, "Air-writing recognition—part ii: Detection and recognition of writing activity in continuous stream of motion data," *IEEE Transactions on Human-Machine Systems*, vol. 46, no. 3, pp. 436–444, 2016.
- [3] S. Mitra and T. Acharya, "Gesture recognition: A survey," *IEEE Transactions on Systems, Man, and Cybernetics, Part C (Applications and Reviews)*, vol. 37, no. 3, pp. 311–324, 2007.
- [4] C. Amma, M. Georgi, and T. Schultz, "Airwriting: a wearable handwriting recognition system," *Personal and ubiquitous computing*, vol. 18, no. 1, pp. 191–203, 2014.
- [5] J. Liu, Z. Wang, L. Zhong, J. Wickramasuriya, and V. Vasudevan, "uWave: Accelerometer-based personalized gesture recognition and its applications," in *2009 IEEE International Conference on Pervasive Computing and Communications*, 2009, pp. 1–9.

- [6] D.-W. Kim, J. Lee, H. Lim, J. Seo, and B.-Y. Kang, "Efficient dynamic time warping for 3D handwriting recognition using gyroscope equipped smartphones," *Expert systems with applications*, vol. 41, no. 11, pp. 5180–5189, 2014.
- [7] D. Lu, K. Xu, and D. Huang, "A data driven in-air-handwriting biometric authentication system," in *2017 IEEE International Joint Conference on Biometrics (IJCB)*, 2017, pp. 531–537.
- [8] S. Patil, D. Kim, S. Park, and Y. Chai, "Handwriting recognition in free space using WIMU-based hand motion analysis," *Journal of Sensors*, 2016.
- [9] M. Alam, K.-C. Kwon, M. Y. Abbass, S. M. Imtiaz, N. Kim *et al.*, "Trajectory-based air-writing recognition using deep neural network and depth sensor," *Sensors*, vol. 20, no. 2, p. 376, 2020.
- [10] L. Ardüser, P. Bissig, P. Brandes, and R. Wattenhofer, "Recognizing text using motion data from a smartwatch," in *2016 IEEE International Conference on Pervasive Computing and Communication Workshops (PerCom Workshops)*, 2016, pp. 1–6.
- [11] C. Amma and T. Schultz, "Airwriting: Bringing text entry to wearable computers," *XRDS*, vol. 20, no. 2, p. 50–55, Dec. 2013. [Online]. Available: <https://doi.org/10.1145/2540048>
- [12] S. Xu and Y. Xue, "Air-writing characters modelling and recognition on modified CHMM," in *2016 IEEE International Conference on Systems, Man, and Cybernetics (SMC)*. IEEE, 2016, pp. 001 510–001 513.
- [13] Y. Li, H. Zheng, H. Zhu, H. Ai, and X. Dong, "Cross-people mobile-phone based airwriting character recognition," in *2020 25th International Conference on Pattern Recognition (ICPR)*. IEEE, 2021, pp. 3027–3033.
- [14] S. Xu, Y. Xue, X. Zhang, and L. Jin, "A novel unsupervised domain adaptation method for inertia-trajectory translation of in-air handwriting," *Pattern Recognition*, vol. 116, p. 107939, 2021.
- [15] C. Li, C. Xie, B. Zhang, C. Chen, and J. Han, "Deep fisher discriminant learning for mobile hand gesture recognition," *Pattern Recognition*, vol. 77, pp. 276–288, 2018.
- [16] P. Roy, S. Ghosh, and U. Pal, "A CNN based framework for unistroke numeral recognition in air-writing," in *2018 16th international conference on frontiers in handwriting recognition (ICFHR)*. IEEE, 2018, pp. 404–409.
- [17] L. Jing, Z. Dai, and Y. Zhou, "Wearable handwriting recognition with an inertial sensor on a finger nail," in *2017 14th IAPR International Conference on Document Analysis and Recognition (ICDAR)*, vol. 1. IEEE, 2017, pp. 1330–1337.
- [18] T. Yanay and E. Shmueli, "Air-writing recognition using smart-bands," *Pervasive and Mobile Computing*, vol. 66, p. 101183, 2020.
- [19] A. Levy, B. Nassi, Y. Elovici, and E. Shmueli, "Handwritten signature verification using wrist-worn devices," *Proc. ACM Interact. Mob. Wearable Ubiquitous Technol.*, vol. 2, no. 3, Sep. 2018.
- [20] H. Wen, J. Ramos Rojas, and A. K. Dey, "Serendipity: Finger gesture recognition using an off-the-shelf smartwatch," in *Proceedings of the 2016 CHI Conference on Human Factors in Computing Systems*, ser. CHI '16. New York, NY, USA: Association for Computing Machinery, 2016, p. 3847–3851.
- [21] A. Graves and J. Schmidhuber, "Offline handwriting recognition with multidimensional recurrent neural networks," *Advances in neural information processing systems*, vol. 21, pp. 545–552, 2008.
- [22] Y. Li, K. Yao, and G. Zweig, "Feedback-based handwriting recognition from inertial sensor data for wearable devices," in *2015 IEEE International Conference on Acoustics, Speech and Signal Processing (ICASSP)*, 2015, pp. 2269–2273.
- [23] X. Lin, Y. Chen, X.-W. Chang, X. Liu, and X. Wang, "SHOW: Smart handwriting on watches," *Proceedings of the ACM on Interactive, Mobile, Wearable and Ubiquitous Technologies*, vol. 1, no. 4, pp. 1–23, 2018.
- [24] D. Moazen, S. A. Sajjadi, and A. Nahapetian, "Airdraw: Leveraging smart watch motion sensors for mobile human computer interactions," in *2016 13th IEEE Annual Consumer Communications Networking Conference (CCNC)*, pp. 442–446.
- [25] P. Khosla, P. Teterwak, C. Wang, A. Sarna, Y. Tian, P. Isola, A. Maschinot, C. Liu, and D. Krishnan, "Supervised contrastive learning," *arXiv preprint arXiv:2004.11362*, 2020.
- [26] Y. Ganin, E. Ustinova, H. Ajakan, P. Germain, H. Larochelle, F. Laviolette, M. Marchand, and V. Lempitsky, "Domain-adversarial training of neural networks," *The journal of machine learning research*, vol. 17, no. 1, pp. 2096–2030, 2016.
- [27] M. Ghifary, W. B. Kleijn, M. Zhang, D. Balduzzi, and W. Li, "Deep reconstruction-classification networks for unsupervised domain adaptation," in *European conference on computer vision*. Springer, 2016, pp. 597–613.
- [28] B. B. Damodaran, B. Kellenberger, R. Flamary, D. Tuia, and N. Courty, "Deepjdot: Deep joint distribution optimal transport for unsupervised domain adaptation," in *Proceedings of the European Conference on Computer Vision (ECCV)*, 2018, pp. 447–463.
- [29] "Noraxon ultium EMG," <https://www.noraxon.com/our-products/ultium-emg/>, accessed: 09-10-2021.
- [30] L. McInnes, J. Healy, and J. Melville, "UMAP: Uniform manifold approximation and projection for dimension reduction," *arXiv preprint arXiv:1802.03426*, 2018.

V. SUPPLEMENTARY MATERIAL

A. Data Collection Setup

In this section, we present sample data collection setup depicted in Figure 3. The figure depicts front and side views of a male subject during the process of airwriting. The IMU sensor used to acquire accelerometer and gyroscope signals is placed on the wrist. For providing a visual feedback of the alphabet that is to be written and also automatically annotating the recordings, a user interface built using the Tkinter module in python was used.



Fig. 3: Depiction of the data collection setup. The IMU sensor placed on the wrist is depicted in the bounding box. The user interface operated by the subject’s left hand is seen on the laptop screen.

B. Visualization of the Feature Space

In this section, we visualize the feature space vectors z , which are the output of the projection head. The 128 dimensional vectors are reduced to 2 dimensions by using Uniform Manifold Approximation and Projection (UMAP) [30].

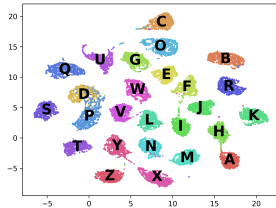


Fig. 4: Scatter plot depicting clusters corresponding to each of the 26 alphabets obtained by applying dimensionality reduction using UMAP on the latent embedding vector

C. Most Confusing Letter Pairs

In this section, we present the top-5 such pairs for different experiment settings in tables 7 to 10. The observations in these tables are also supported by Figure 4 as it can be seen that the clusters for the most confusing pairs are close to each other in the latent space.

Table 7: The 5 most confusing for LOSO experiments on source dataset.

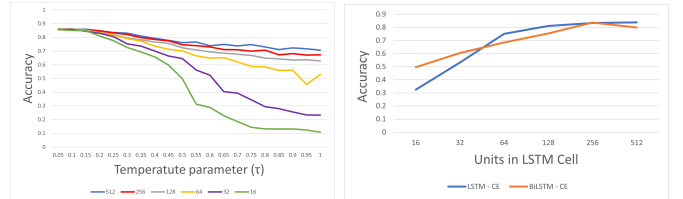
Rank	Letters Pair	% of Total Error
1	D,P	15.06%
2	F,I	5.97%
3	X,Y	3.75%
4	N,W	3.39%
5	C,O	2.34%

Table 8: The 5 most confusing for LOSO experiments on target dataset.

Rank	Letters Pair	% of Total Error
1	D,P	13.51%
2	X,Y	4.87%
3	G,O	4.45%
4	N,W	4.32%
5	G,Q	4.18%

D. Effect of Hyperparameters

We analyze the effect of changing the parameters of the supervised contrastive loss on the classification performance. We changed the temperature parameter, $\tau \in \{0.05, 0.1, \dots, 0.95, 1\}$ and the dimension of the projection encoding, $D_P \in \{512, 256, 128, 64, 32, 16\}$. The mean accuracies achieved on LOSO experiments on the source dataset using the 1DCNN model are presented in Figure 5a. The variation of mean recognition accuracies with respect to the number of units in LSTM cell using CE loss for the LSTM and BiLSTM architectures are presented in Figure 5b. We also vary the number of filters for the first couple of convolution layers (N_1) and for the later layers (N_2), and the filter length, the effects of which on the classification performance are presented in Figure 6.



(a) Mean recognition accuracy vs. τ and (b) Mean recognition accuracy vs. units in LSTM cells.

Fig. 5: Variation of mean recognition accuracy.

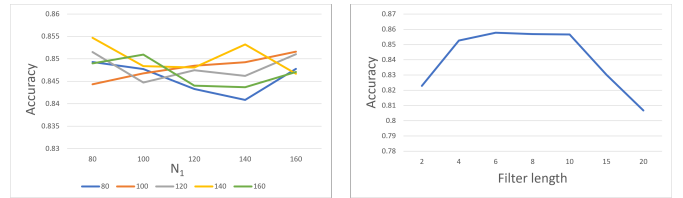


Fig. 6: Variation of accuracy by changing the number of filters (N_1 and the variation of N_2 is shown with different colors) and filter length for the 1DCNN architecture.

E. Comparison with AdaBN

In this section, we compare the proposed approach with AdaBN as in [13]. For this task, we randomly selected 50% of the subjects from the target dataset as a test set (2600 samples) and the remaining 50% of the subjects from the target dataset were used for domain adaptation. We set up the experiment using the 1D-CNN architecture as described in the paper in both supervised and unsupervised settings and the results are presented in Table 11.

Table 11: Comparison of the proposed approach with AdaBN

Setting	AdaBN	CE	SCL
Unsupervised	0.6096	0.7403	0.7723
Supervised	0.7196	0.7746	0.8046

Table 9: The 5 most confusing target pairs with the model trained on the source data

Rank	Letters Pair	% of Total Error
1	D,P	9.88%
2	X,Y	7.61%
3	G,Q	7.51%
4	F,I	3.75%
5	N,W	3.66%

Table 10: The 5 most confusing target pairs with a pre-trained model fine-tuned on target data

Rank	Letters Pair	% of Total Error
1	D,P	14%
2	X,Y	5.86%
3	N,W	4.43%
4	G,Q	4.28%
5	M,N	3.86%